1 OF 1
AD
A059000

END
DATE
FILMED
11-78
DDC

MICROCOPY RESOLUTION TEST CHART

NATIONAL BUREAU OF STANDARDS-1963-A

LEVEL II

②

TRANSPORT PROPERTIES OF METAL OXIDES IN THE PRESENCE OF SULFUR

Final Scientific Report

January 1, 1975 through December 31, 1977

Contract F44620-75-C-0043

Prepared for

Electronic and Solid State Sciences
Air Force Office of Scientific Research
Bolling Air Force Base
Washington, DC 20332

by

H.S. Spacil and D.A. Shores
General Electric Company
Corporate Research and Development
Schenectady, New York 12301

D D C

SEP 25 1978

June 1978

SRD-78-081

78 07 20 153

REPORT DOCUMENTATION PAGE		READ INSTRUCTIONS BEFORE COMPLETING FORM
1. REPORT NUMBER AFOSR-TR-78-1144	2. GOVT ACCESSION NO.	3. RECIPIENT'S CATALOG NUMBER
4. TITLE (and Subtitle) TRANSPORT PROPERTIES OF METAL OXIDES IN THE PRESENCE OF SULFUR.		5. TYPE OF REPORT & PERIOD COVERED Final Scientific Report - 1 Jan 1975 - 31 Dec 1977
		6. PERFORMING ORG. REPORT NUMBER SRD-78-081
7. AUTHOR(s) H.S. Spacil and D.A. Shores		8. CONTRACT OR GRANT NUMBER(s) F44620-75-C-0043
9. PERFORMING ORGANIZATION NAME AND ADDRESS General Electric Company Corporate Research and Development Schenectady, New York 12301		10. PROGRAM ELEMENT, PROJECT, TASK AREA & WORK UNIT NUMBERS 61102F 2306/A2
11. CONTROLLING OFFICE NAME AND ADDRESS Electronic and Solid State Sciences / NE Air Force Office of Scientific Research Bolling Air Force Base, DC		12. REPORT DATE June 1978
		13. NUMBER OF PAGES 53
14. MONITORING AGENCY NAME & ADDRESS(if different from Controlling Office)		15. SECURITY CLASS. (of this report) Unclassified
		15a. DECLASSIFICATION/DOWNGRADING SCHEDULE

16. DISTRIBUTION STATEMENT (of this Report)

APPROVED FOR PUBLIC RELEASE; DISTRIBUTION UNLIMITED

17. DISTRIBUTION STATEMENT (of the abstract entered in Block 20, If different from Report)

18. SUPPLEMENTARY NOTES

19. KEY WORDS (Continue on reverse side if necessary and identify by block number)

hot corrosion, sulfidation, oxide films, diffusion, conductivity

20. ABSTRACT (Continue on reverse side if necessary and identify by block number)

The electrical conductivities of polycrystalline NiO, single crystal NiO, and single crystal CoO were measured to determine: (1) the effect of SO_2 in O_2 - SO_2 mixtures on conductivity, and (2) the effect of exposure to SO_2 on defect diffusivity. Only the single crystal oxides proved to be satisfactory for measurement. Small conductivity increases of the order of 1% were found on exposure to SO_2. Diffusivity measurements agreed well with literature values for sulfur-free specimens, and indicated the presence of a sulfur-induced defect

(continued on back)

DD FORM 1473 EDITION OF 1 NOV 65 IS OBSOLETE
1 JAN 73

(20. cont'd)

having a diffusivity no more than an order of magnitude less than that of cation vacancies in specimens that had been exposed to SO_2. Mechanisms that might cause an increase in sulfur activity or chemical potential during oxidation of metals are considered. A sulfur-induced defect consisting of $S^{(+)}$ ions on cation sites is postulated as being consistent with the observations, and it is shown that such a defect can lead to an increase in sulfur activity at the metal/oxide interface of a growing oxide. Supplementary thermogravimetric measurements indicated a sulfur solubility in CoO of about 0.05 mole percent.

D D C
RECEIVED
SEP 25 1978
D

Transport Properties of Metal Oxides

In the Presence of Sulfur

H. S. Spacil and D. A. Shores

I. INTRODUCTION

The work described in this report has been addressed to the effects of sulfur on the oxidation of metals by gases. As distinct from the type of oxidation known as "hot corrosion", and which involves formation of condensed sulfur-containing salts on the metal surface, acceleration of oxidation rates of many metals can occur in atmospheres which contain O_2 but also contain the oxidized sulfur-bearing species SO_2 and SO_3. This acceleration occurs when the chemical activity or potential of oxygen in the atmosphere is sufficient to form the metal oxide MO_x while the activity or potential of sulfur is too low to support formation of the sulfide MS_y from a thermodynamic standpoint.* Two general classes of sulfur effects have been observed for metals which normally form compact, protective oxide scales in O_2: either a compact oxide scale is formed, but with a rate constant which increases with sulfur content of the atmosphere, or a duplex oxide/ sulfide scale is formed, often at a rate much higher than that of simple oxidation alone. In the former

---

*The chemical activities a_0 and a_S of oxygen and sulfur are defined in terms of the equilibrium partial pressures, p_{O_2} and p_{S_2}, as $(p_{O_2}/p°)$ and $(p_{S_2}/p°)^{1/2}$, respectively, where $p°$ is the pressure chosen for the reference state (usually 101.3 kPa or 1 atm.). The chemical potentials μ_0 and μ_S are defined as $RT \ln (a_0)$ and $RT \ln (a_S)$, respectively, where R is the gas constant in Mj/kg-mole/°K and T is the absolute temperature in °K. Units of μ_0 and μ_S are then Mj/kg-mole or kj/gram-mole.

situation, metallographic examination of the scale often shows the presence of sulfide at the metal/scale interface. Thus sulfur effects on oxidation can be linked to an increase in sulfur activity or potential to values above those corresponding to thermodynamic equilibrium in the atmosphere to which the metal is exposed. In general, oxidation rates of metals subject to such effects are determined by transport of metal cations through the oxide scale; once a duplex oxide/sulfide scale forms, the much faster transport of cations through the sulfide portion of the scale would indeed be expected to result in metal attack at rates higher than for simple oxidation. The metals iron, nickel, and cobalt, as well as their technologically important oxidation-resistant alloys, all are subject to sulfur effects in oxidizing atmospheres. Understanding the nature of the increase in sulfur activity during oxidation would provide a basis for its control or suppression.

Prior work by various investigators has suggested three possible mechanisms for observed sulfur effects on oxidation:

1) Surface reaction rates at the scale/gas interface limit the rate of transfer of oxygen from the atmosphere to the scale, resulting (under the proper conditions) in an increase of sulfur activity at the scale surface; 2) Gas phase transport through a boundary layer of gas adjacent to the scale surface depletes the oxygen content of gas within this layer, leading to an increase of sulfur activity in the gas at the scale surface; and 3) Sulfur transport through the scale itself either allows sulfur to: (a) reach a region within the scale where the oxygen activity has decreased to a level which allows sulfide formation, or (b) results in an

increase of sulfur activity to a level which likewise allows sulfide

formation.

Each of these three mechanisms will be discussed in more detail in

Section IV. The present work was concerned principally with the third

mechanism. It was originally proposed to measure the electrical con-

ductivity of metal oxides at known oxygen and sulfur activities. Iron,

nickel, cobalt, and probably chromium oxides are metal deficit, p-type

electrical conductors in which cation vacancies are the principal

defect. The prototypical equilibrium of cation vacancies and electron

holes in the oxide MO with oxygen can be written as

$$1/2 \ O_2 \ (g) \ \overset{\rightarrow}{\leftarrow} \ O^= \Big| {}^x_0 + V'_M + h^{\cdot}$$
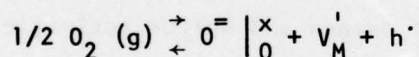
where, in slightly modified Kroger-Vink notation, $O^= \Big| {}^x_0$ is a doubly

(negative) charged oxygen ion on an anion site with zero excess charge,

V'_M is a cation vacancy with a single negative excess charge, and $h^{\cdot}$ is

an electron hole with a single positive excess charge. In an intrin-

sically conducting oxide, conductivity at a fixed temperature is a

measure of the highly mobile electron hole concentration. If sulfur

were to enter the oxide with a non-zero excess charge as an electron

donor or acceptor, a conductivity change would result from the resultant

change in electron hole concentration. Any such change would also imply

a change in the cation vacancy concentration, which might explain the

increase of oxidation rate caused by sulfur even when no duplex oxide/sulfide

scale is formed during oxidation.

In practive, the absolute conductivity need not be measured to determine relative conductivity changes. The admittance Y of a specimen, equal to the ratio of current to voltage, can be used to define a function ϕ' as

$$\phi' = (Y-Y^i)/Y^i \qquad \qquad I-1$$

where Y^i is the initial admittance. Any change in ϕ' is simply the relative change in conductivity and thus of electron hole concentration.

Measurements of ϕ' for NiO and CoO subjected to experimentally obtainable combinations of oxygen and sulfur activities showed changes of the order of 1% in the presence of sulfur. These measurements, and their significance, will be discussed in detail in Section III. In view of the small measurable effect, the experimental program was modified to allow measurement of the defect diffusivity of oxide specimens containing sulfur. A step change in O_2 partial pressure over an oxide causes a corresponding change in the surface cation vacancy concentration. As vacancies subsequently diffuse in or out of the oxide to reach the new equilibrium value, both the admittance Y and the mass M of the oxide will change with time. The normalized change of either is given by the function ϕ, defined as

$$\phi = (Y-Y^f)/(Y^i-Y^f) = (M-M^f)/(M^i-M^f) \qquad \qquad I-2$$

where the superscript i indicates the initial value, and as before, the superscript f indicates the final value, and Y and M are the transient admittance and mass. Analysis of the variation of ϕ vs. time can yield diffusivity values for specimens of known geometry. These diffusivities are unambiguous if a single mobile entity is diffusing via a single process; changes in either the diffusion process or the nature of the diffusing entity lead to multiple diffusivities which may be separable if their respective time constants differ sufficiently. An advantage of diffusivity measurements is then the detection of low-level effects, subject to the restriction of time constant difference. Such effects were found for both NiO and CoO.

The possible effects of sulfur dissolved in a metal oxide on oxidation rate and sulfur activity gradients through the oxide were also considered theoretically. Since electron holes and lattice defects carry an excess charge, the local electrical potential must be considered in the formulation of appropriate transport equations. This was done for a model of a growing oxide scale, allowing two different types of sulfur-induced defects in the oxide. One assumed set of defect properties can be shown to lead to increases in both oxidation rate and sulfur activity at the metal/scale interface. A surprising implication of this situation, however, is that cation vacancies diffuse up their own concentration gradient, due to the coupling between transport of various defects and electron holes through the local electrical potential. Changes in cation vacancy concentration of a metal oxide due to the

presence of an added component such as sulfur may then not be sufficient in themselves to explain changes in oxidation rate.

II. Experimental

A. NiO

1) Polycrystalline NiO

Cylindrical specimens were prepared by sintering high purity NiO powder in oxygen at temperatures to 1800°C. These had greater than 95% of theoretical density, and could be ground to a diameter of 0.635 cm (0.25 in). Platinum electrodes were applied to allow 4-point admittance measurements.

A zirconia electrolyte EMF cell was utilized to monitor the instantaneous equilibrium O_2 partial pressure over the specimen during transient measurements in which the admittance change with time is obtained following a change in nominal O_2 pressure.

2) Single Crystal NiO

A prismatic single crystal about 0.098 cm on each face by 0.7 cm in length was obtained, with a total metallic impurity level of 80 ppm or less*. The source material had shown essentially intrinsic conductivity behavior at high temperatures, and could thus be considered free of impurities at a level that would lead to extrinsic conduction. Platinum electrodes were applied to allow 4-point admittance measurements, but the EMF cell utilized with the polycrystalline specimens was not employed for this specimen. It was expected that diffusional time constants

*Atomergic Chemetals Corp., Plainview, N.J.

would be much greater than those for equilibrium O_2 or S_2 partial
pressure changes, and this condition appears to have been satisfied.

A series of three runs at 1000°C on this specimen will be dis-
cussed. The description of these runs is:

Run A. Specimen equilibrated in CO_2 with O_2 pressure of 10^{-4} atm;
O_2 pressure changed to 1 atm and transient admittance measured.

Run B. Specimen equilibrated in O_2-10%CO_2; gas changed to O_2-
10%SO_2 and transient conductivity measured.

Run C. Specimen equilibrated in O_2-10%SO_2; gas changed to CO_2 with
O_2 pressure of 10^{-4} atm for 105 minutes; O_2 pressure changed to 1 atm
and transient admittance measured.

B.   CoO

Prismatic single crystals about 0.2 cm on each face and from 1.2
to 1.8 cm in length were obtained, with a total metallic impurity level
of 380 ppm or less*. The major impurity was Fe (200 ppm). This impurity
level should ensure intrinsic conduction at high temperatures since the
cation vacancy concentration of CoO is of the order of 10^{-3} at 1000°C
for an O_2 partial pressure of 1 atm. All measurements were made at
1000°C and 1 atm total pressure.

1) Admittance Measurements

Four different atmospheres were used to provide step changes in O_2
partial pressures: O_2, 90% O_2 - Ar, air, and CO_2 with an O_2 partial
pressure of 10^{-4} atm. Transient admittance measurements were made for
five different combinations of initial and final atmospheres on several
sulfur-free specimens, as shown in Table II.1.

---

*Atomergic Chemetals Corp., Plainview, N.J.

Table II.1

| INITIAL | | FINAL | | |
	O_2	90% O_2 - Ar	Air	CO_2
90% O_2 - Ar	-	-	X	-
Air	X	X	-	X
CO_2	-	-	X	-

Transient admittance measurements were then made on three crystals for the conditions given in Table II.2.

Table II.2

Run	Initial Atmosphere	Equilibration Time	Final Atmosphere	
8	90% O_2 - Ar	100 hrs	90% O_2 - SO_2	
1	90% O_2 - SO_2	50 hrs	Air	Same
12	Air		O_2	
13	O_2		Air	Specimen
16	90% O_2 - SO_2	50 hrs	Air	

2) Mass Measurements

Three different atmospheres were used to provide step changes in O_2 partial pressures: O_2, air, and Ar with an O_2 partial pressure estimated at 10^{-5} atm. Transient mass measurements were made for three different combinations of initial and final atmospheres on one specimen, as shown in Table II.3.

Table II.3

	INITIAL	FINAL
	O_2	Ar
O_2	-	X
Air	X	-
Ar	X	-

The same specimen was equilibrated with O_2, then exposed to a 98% O_2-SO_2 atmosphere for 125 hrs, and the resultant weight change measured. A final transient mass measurement was made after equilibration with O_2 and a change to an Ar atmosphere.

III. Experimental Results

Mathematical expressions for the time dependence of the function, ϕ, applicable to cylindrical or prismatic specimens, are well-known[1]. Where a single mobile entity is diffusing with a concentration-independent diffusivity, these expressions can be employed to determine the diffusivity by numerical or graphical techniques. For a metal-deficit metal oxide in which cation vacancy diffusion dominates the time dependence of ϕ, the measured diffusivity will be the chemical interdiffusion coefficient $\tilde{D}$. The requirement for local electroneutrality within the oxide leads to a relation between $\tilde{D}$ and the vacancy diffusivity D_V, which can be expressed as

$$D_V = \tilde{D}/(1 + n)$$

III-1

where n is the excess (negative) charge on the vacancy[2]. Further, the self-diffusion coefficient for the metal, D_M, is related to D_V through the relationship

$$D_M = x_V D_V \qquad\qquad III-2$$

where x_V is the fraction of cation sites occupied by vacancies[2]. Independent measurements of $\tilde{D}$, D_M, and n on several oxides have confirmed these relations as valid under conditions where the principal defects are cation vacancies. Since the NiO and CoO specimens used in the present work should meet this criterion, transient admittance or mass measurements then yield $\tilde{D}$.

A) NiO Admittance Measurements

1) Polycrystalline NiO

EMF cell voltages showed that the time constant for an O_2 partial pressure change in the vicinity of the specimen was of the order of 100 seconds, even when changing from low to high values. Such a change is clearly not a step change, but will not be significant if the time constant for admittance changes is much greater. The time constant for the latter was of the same order of magnitude, however, indicating that the specimen conductivity was following the O_2 partial pressure change fairly closely.

The driving force for conductivity changes is the surface concentration of vacancies, $x_V^{(s)}$, which in turn will be proportional to the $1/(1 + n)$ power of the oxygen activity at the oxide surface. A normalized surface vacancy concentration is given by the function Φ, defined as

$$\Phi = (x_V^{(s)} - x_V^{(s),f})/(x_V^{(s),i} - x_V^{(s),f}) \qquad \text{III-3}$$

where the superscripts i and f have the same meaning as in I-2. The value of Φ can be obtained readily from EMF cell voltage for any appropriate value of n. For intrinsically conducting NiO, n will be 1 for singly charged (negative) nickel vacancies and 2 for doubly charged nickel vacancies. Figure 1 shows a typical plot of ϕ (solid line) and Φ (dashed line) for polycrystalline NiO at 800°C on changing the equilibrium O_2 pressure from 10^{-4} to 1 atm. A value of 2 was taken for n to obtain Φ, but a value of 1 does not change the shape or values of Φ significantly. The points shown along the solid line of Fig. 1 are not experimental points, but represent calculated values of ϕ at specific times as will be discussed subsequently. Note that the function ϕ lags the surface vacancy concentration function Φ as would be expected, but that the lag can be substantially less than the total time elapsed. Thus a simplified interpretation of normalized conductivity changes to obtain $\tilde{D}$ is not possible.

For a cylindrical specimen the function ϕ can be expressed readily in terms of the normalized surface vacancy concentration as

$$\phi = \Phi - 4 \sum_{k=1}^{\infty} \frac{\int_0^t \left.\frac{d\Phi}{dt}\right|_{t'} \exp\left(-w_k^2 \frac{t-t'}{\tau}\right) dt'}{w_k^2} \qquad \text{III-4}$$

where t is the time of measurement, t' is a variable of integration, and the dimensionless quantity w_k is the kth root of the zero-order Bessel function of the first kind. The time constant τ is the ratio $r^2/\tilde{D}$, where r is the specimen radius[1].

Equation III-4 involves the derivative of an experimentally determined quantity, i.e., Φ. An alternative expression involving Φ directly can be obtained through integration as

$$\phi = 4 \sum_{k=1}^{\infty} \left[\frac{\exp\left(-w_k^2 \frac{t}{\tau}\right)}{w_k^2} + \frac{1}{\tau} \int_0^t \left.\Phi\right|_{t'} \exp\left(-w_k^2 \frac{(t-t')}{\tau}\right) dt' \right] \qquad \text{III-5}$$

Since all quantities in III-5 are known except τ, the latter can be treated as an unknown for any pair of values of ϕ and t. This was done numerically for the data of Fig. 1 at ϕ at 0.5 and t = 134 sec, yielding a value for τ of 980 sec. As a check on the validity of this value, it was used to calculate ϕ at the seven other points shown on Fig. 1. The agreement of the calculated points with the shape of the experimentally determined plot indicates that III-5 correctly describes the conductivity variation with time and surface vacancy concentration. The use of an EMF cell can therefore allow determination of time constants for diffusion even when these are comparable to the time constant for the equilibrium O_2 pressure changes governing surface vacancy concentrations. It may be noted that the parameter n could also

be treated as an unknown, thus in principle allowing a determination of net vacancy charge. In the present treatment of the data, a value of 2 for n gave better agreement of calculated and measured conductivities than a value of 1, but the subject was not investigated in detail.

The diffusional time constant of 980 sec and specimen radius of 0.318 cm yield a vacancy diffusivity of 3.5×10^{-5} cm^2/sec. Literature data indicate that a value of the order of 10^{-8} cm^2/sec might be expected at 800°C for bulk (single crystal) diffusion[3]. Either grain boundary diffusion or gas phase transport of oxygen through pores may be responsible for the high diffusivity obtained; the latter is suggested as more probable. The polycrystalline NiO specimens were prepared from powder with a grain size estimated at 100 μm. If diffusion were occurring into cylinders with a 50 μm radius, the diffusional time constant of 980 sec leads to a vacancy diffusivity of about 10^{-8} cm^2/sec, suggesting that this process may actually be taking place. The high apparent diffusivity obtained appears in any event to be an artifact of the specimen structure. While it may be possible to correlate the apparent diffusivity with bulk defect properties, this cannot be done with certainty. Attempts to measure and characterize sulfur effects on conductivity in polycrystalline NiO are then unwarranted unless structural factors are better understood.

2)   Single Crystal NiO

The three runs made on the single crystal specimen had these specific objectives. Run A was designed to obtain the vacancy diffusivity in the absence of sulfur. Run B was designed to maintain the O_2 pressure nearly

constant, but to vary the equilibrium S_2 pressure and determine any
conductivity changes due to sulfur-induced defects. Run C was designed
to introduce sulfur into the specimen, then obtain the vacancy dif-
fusivity while some sulfur still remained in the specimen.

Considering run B first, Fig. 2 is a plot of the relative con-
ductivity function ϕ', as defined in I-1, vs. time. This figure shows
an initial decrease in conductivity, followed by an increase starting
after about 25 minutes. The conductivity stabilized after several
hundred minutes at some value greater than the initial value, then
underwent changes with relatively short time constants that are most
probably associated with variations in experimental conditions. The
O_2 - 10% SO_2 mixture was obtained by mixing the two constituent gases;
slight changes in the flow rate of either would cause corresponding
changes in the O_2 partial pressure, and thus in conductivity. Flow rate
or compositional changes which affect gas mixture thermal conductivity will
cause corresponding changes in specimen temperature and in specimen
conductivity. And the change from an initial O_2 - CO_2 atmosphere to an
O_2 - SO_2 atmosphere would also be expected to change specimen temperature
due to the different thermal conductivities of these two mixtures. The
heat of activation for conduction in NiO is about 96 kj, so that a 1°C
temperature change of the specimen would lead to relative conductivity
change of about 0.8% at 1000°C. While Fig. 2 shows a relative conductivity
increase of as much as 8%, it is estimated that variations in experimental
conditions may lead to relative conductivity changes of 3 to 4%. Thus
the final relative conductivity increase in NiO on changing from O_2 -
CO_2 to O_2 - SO_2 may be at most of the order of a few percent.

The normalized conductivity function of a prismatic oxide specimen in which cation vacancy diffusion is occurring following a step change in O_2 partial is given approximately by

$$\ln (\phi) = \ln (\alpha) - t/\tau \qquad \text{III-6}$$

in the range of time t where ϕ is less than about 0.6. In III-6, α is a numerical constant with a value of about 0.8, and the time constant τ is equal to $2a^2/\pi^2\tilde{D}$, where a is one half the prism face width, and $\tilde{D}$ can be calculated.

Normalized conductivity can be obtained for runs A and C in a straightforward manner since conductivity measurements could be carried out for sufficient time after an O_2 pressure change to obtain a value for Y^f. For run B, the value of Y^f is affected by the gas mixing system as mentioned previously. Thus the value of Y^f was taken as the admittance reached during the plateau of Fig. 2 at times of 400-500 minutes. The normalized conductivity for run B will then exceed unity at low times during which the conductivity initially decreases.

Figure 3 is a plot of the normalized conductivity function, on a logarithmic scale, against time for the three runs. Run A shows the expected linear portion with a time constant of 2360 sec which corresponds to a vacancy diffusivity of 5.6×10^{-8} cm^2/sec, assuming a value for n of 2. While different investigators disagree on whether cation vacancies in NiO are singly or doubly charged[3,4], the mole fraction of these is about 5×10^{-5} at 1000°C, leading to a value for the self diffusion

of Ni as 2.8×10^{-12}, within the range reported[5]. The results of
run A were quite reproducible, and indicate diffusion dominated by
cation vacancies.

Run B shows normalized conductivity values exceeding unity at
low times, then a linear portion with a time constant of 3780 sec.
Although run B was carried out at a nominally constant O_2 pressure while
SO_2 was substituted for CO_2, the initial decrease in conductivity
is most probably due to an O_2 pressure change during this substituion.
The linear portion of run B then represents diffusion of a sulfur-
induced defect which increases the conductivity. Interpretation of
run B indicates that sulfur entering NiO increases conductivity, thus
behaving as an electron acceptor, and induces a defect having an apparent
diffusivity of 10^{-7} cm^2/sec. While interpretation of the linear portion
of run B is not straightforward, it is simple to demonstrate that the
normalized conductivity function will be dominated at long times by the
slower of two simultaneous defect diffusion processes provided the
conductivity changes induced by the different defects at those times
are comparable. Figure 2 indicates that this latter criterion is
satisfied, and thus that diffusion of the sulfur-induced defect dominates
run B after about 50 minutes.

Run C shows a linear portion up to about 50 minutes with a time
constant of 2370 sec that can be identified with cation vacancy diffusion.
A change in slope occurs after this time. Since the specimen was held
at a low O_2 pressure, after equilibrating with O_2-10%SO_2 prior to this
run, most of the sulfur-induced defects would be expected to diffuse
out of the specimen during this holding period if the diffusivity obtained

from run B is correct. At long times, however, the remaining sulfur-induced defects might be expected to affect the conductivity. The conductivity was increasing through run C, but the removal of sulfur-induced defects which tend to increase the conductivity would slow down the rate of increase at long times. Thus the direction of the rate of conductivity change of the second linear portion of run C is consistent with the interpretation of run B.

B. CoO Admittance Measurements

At an O_2 partial pressure of 1 atm, CoO has a vacancy mole fraction of about 8×10^{-3} at 1000°C, so its intrinsic conductivity should be less susceptible to effects of metallic impurities than NiO. Also, it is generally agreed that, except at higher temperatures, singly charged cation vacancies are the predominant defect in CoO[6].

1) Oxygen Activity Change in the Absence of Sulfur

When treated according to III-6, admittance data from the runs made as described in Table II.1 of Section II-B-1 yielded values of $\tilde{D}$ ranging from 6.38×10^{-7} to 12.1×10^{-7}, with a mean of 10.0×10^{-7} cm^2/sec. Since n is equal to 1, a vacancy mole fraction of 8×10^{-3} leads to a value for the self-diffusion of Co at 1 atm O_2 partial pressure as 4.0×10^{-9}. This is well within the range reported[5,6], and indicates diffusion governed by cation vacancies.

Results of a typical run are shown in Fig. 4, where the quantity $-\ln(\phi)$ is plotted against time. The experimental points shown in Fig. 4 give a satisfactory fit to a straight line between the limits for ϕ of about 0.6 and 5×10^{-3}. The upper limit is determined by

the approximations inherent in III-6, while the lower limit is deter-
minted by the magnitude of the O_2 partial pressure step change together
with the sensitivity and stability of the admittance measuring cir-
cuitry. The lower limit corresponds to a value for $-\ln(\phi)$ of about
5; measurements out to times leading to this value are felt to be reliable.

2) Sulfur Activity Change at Constant Oxygen Activity

Run 8 as described in Table II.2 of Section II-B-1 allowed
measurement of the relative conductivity change induced by the intro-
duction of sulfur at nominally constant oxygen activity. Results are
presented in Table III.1.

Table III.1

Time (seconds)	$\phi' \times 10^2$
0	0
300	0.81
600	1.01
900	1.42
1200	1.52
1800	1.63
2400	1.73
3000	1.94
3600	2.04
4200	2.25
4800	2.25
5400	2.14
6000	2.04
600 - 25000	2.04 - 2.35

Table III.1 shows a relative conductivity increase of about 2% following
the introduction of SO_2. The same considerations as applied to run B
for single crystal NiO, as discussed in Section III-A-2, apply to run 8

for CoO. Due to a lower heat of activation for conduction in CoO,
it is estimated that variations in experimental conditions may lead
to relative conductivity changes of about 1%. Thus the final relative
conductivity increase in CoO on changing from O_2 - Ar to O_2 - SO_2
may be of the order of 1%.

3)   Oxygen Activity Change in the Presence of Sulfur

Runs 12 and 13 as described in Table II.2 of Section II-B-1 allowed
measurement of the normalized conductivity function for both positive
and negative step changes in oxygen activity following exposure of a
specimen to a sulfur-containing atmosphere. Results of these runs are
shown in Fig. 5; in comparison with Fig. 4, it should be noted that the
time scale of Fig. 5 extends to higher values. An averaged curve is
shown for the two runs in Fig. 5, but each could be separated approximately
into two near-linear segments intersecting at a value for ϕ of about
0.025. This suggests that when the initial conductivity has changed
by about 98%, diffusion of some sulfur-induced defect determines further
conductivity changes. Table III.2 gives the apparent diffusivities
resulting from separation of each curve into two linear segments: these
are designated by D' for short times and D'' for long times.

Table III.2

Run	D' (cm^2/sec)	D'' (cm^2/sec)
12	9.55×10^{-7}	1.21×10^{-7}
13	10.4×10^{-7}	3.25×10^{-7}

If it is assumed that a sulfur-induced defect does increase the conductivity of CoO by a small amount of the order of 1%, then Figs. 6a and 6b show schematically the conductivity variations with time that could give rise to the results of Fig. 5. In each of these two plots, the dashed lines labelled σ_0 and σ_S are the contributions to the total conductivity due to electron holes associated with cation vacancies and the sulfur-induced defect, respectively. The solid line is the total conductivity, which at long times is determined primarily by diffusion of the sulfur-induced defect. The apparent diffusivity D'' at long times will be less for a positive oxygen activity change, as in Fig. 6b where the individual conductivity variations oppose each other, than for a negative oxygen activity change, as in Fig. 6a, where the conductivity variations are in the same direction.

Run 16 was essentially a repeat of run 13, but without the intervening exposure to O_2 of run 12 following exposure to the 90% O_2 - SO_2 atmosphere. The normalized conductivity function could again by separated into two near-linear segments, yielding two apparent diffusivities with D' having a value of 9.28×10^{-7} cm^2/sec.

The values of D' obtained in runs 12, 13 and 16 are in good agreement with the chemical interdiffusion coefficient obtained in the absence of sulfur. The short time variation in the normalized conductivity function then can be ascribed to cation vacancy diffusion. Since the change to a lower apparent diffusivity occurs for values of $-\ln(\phi)$ less than 5, this change is considered to be a reliable indication of an increase of conductivity associated with a sulfur-induced

defect whose apparent diffusivity is about 5 times less than that of cation vacancies.

C.   CoO Mass Measurements

A Cahn RG thermobalance and digital data recording system were used to carry out the measurements described in Section II-B-2.   The requirement for a flowing atmosphere over the specimen, however, caused a high noise level in the analog signal from the thermobalance control circuit.   Data points taken by the data recording system at discrete times were recorded and subsequently computer processed by averaging over an arbitrary number of adjacent points (usually either 5 or 10). This averaging removes some of the information associated with the normalized mass function defined by I-2, since if carried to an extreme, it will simply generate the average value of ϕ over the time of the experiment.   Values of $-\ln(\phi)$ do not appear to be reliable above 3, and results obtained are felt to be less significant than those obtained from admittance measurements.

Step changes of oxygen activity in the absence of sulfur, as described in Table II.3 of Section II-B-2, resulted in averaged data yielding values for the chemical interdiffusion coefficient of about 28×10^{-7} cm^2/sec when treated according to III-6.   The discrepancy between this value and that from admittance measurements may be due in large part to the averaging technique.   Following exposure to a 98% O_2 - SO_2 atmosphere and then to O_2, the specimen was subjected to a negative step change in oxygen activity.   An average apparent diffusivity for this run was 15×10^{-7} cm^2/sec, suggesting that a slower diffusion process was influencing the apparent diffusivity.

Thermobalance data did allow determination of the long time mass gain of the specimen after changing from an O_2 atmosphere to a 98% O_2 - SO_2 atmosphere. Since the rate of change of mass is not important in such a measurement, data point averaging will improve the result. Bouyancy corrections for the difference in density of the two atmospheres allow a determination of the actual mass gain of the 0.46 gram specimen as 0.094 milligrams. This increase corresponds to a sulfur mole fraction of about 5×10^{-4}.

IV. Discussion

Other investigators have concluded that sulfur dissolved in NiO either decreases conductivity[7] or has no effect on conductivity[8]. The self-diffusion coefficient of sulfur in NiO and CoO has been reported as about two orders of magnitude less than the self diffusion coefficient for the respective metals[7]. The present work indicates that exposure to an atmosphere containing 10% SO_2 increases the conductivity of NiO and CoO slightly, at least at high O_2 partial pressures, and that some sulfur-induced defect in these oxides has an apparent diffusivity no more than an order of magnitude less than the chemical interdiffusion coefficient due to cation vacancies. For CoO at 1000°C and 1 atm O_2, the mole fraction of dissolved sulfur due to exposure to an atmosphere containing 2% SO_2 is 5×10^{-4}, or about 6% of the cation vacancy concentration. The sulfur activity of these O_2 - SO_2 mixtures is of the order of 10^{-11}. Even at such a low sulfur activity, our results suggest that a significant amount of sulfur can be dissolved in a metal-deficit oxide, but that only a small fraction of this sulfur affects the electron

hole or vacancy concentration at high O_2 partial pressures.

To consider whether the results of the present work are consistent with observed sulfur effects on oxidation, it is useful to employ the reaction path concept of the possible activities or chemical potentials that may arise during oxidation. This concept, as applied to sulfur effects on oxidation, utilizes the stability diagram for the M-O-S system; such a diagram is simply a phase diagram depicting regions of metal, oxide, and sulfide stability in terms of oxygen and sulfur activities or chemical potential rather than composition. The locus of all possible simultaneous values of oxygen and sulfur activities encountered during oxidation (the "reaction path" is superimposed on the stability diagram to explain or predict the existence of observed phases. Reaction paths have been presented by several investigators in connection with all three of the mechanisms for sulfur effects on oxidation summarized in Section I[9,10,11]. In general, as stated in Section I, the objective of such an approach is to ascertain whether increases in sulfur activity can occur during metal oxidation.

A. Surface Reaction Rate

The reaction path concept is least helpful here since surface reaction rate limitation of scale-forming reactions implies discontinuities in oxygen or sulfur activities, or both, at the scale/gas interface. Surface reaction rate limitation of sulfide formation on Fe has been demonstrated, but only in atmospheres where sulfides were thermodynamically stable [12]. A slow adsorption process at the scale surface,

for example, can lead to surface reaction rate limitation of scale
formation. For formation of duplex oxide/sulfide scale, surface reaction
rates would have to affect both oxygen and sulfide activities at the
scale surface, especially in atmospheres with a high O_2 partial
pressure: the oxygen activity would have to decrease, while the sulfur
activity would have to simultaneously increase. Since duplex scale
formation is observed on several different metals and alloys, this
characteristic of surface reaction rates would have to apply to a variety
of oxide or oxide/sulfide surfaces. In view of the highly specific
nature of surface reaction rate kinetics, this wide applicability seems
unlikely.

B. Gas Phase Transport

Any solid metal exposed to a flowing atmosphere will have a mass
transport boundary layer of gas adjacent to its surface. The gas
velocity will decrease throughout this layer, becoming essentially
zero at the solid surface. Diffusive transport of oxygen and sulfur
must occur through this layer for oxide and sulfide to form. If oxygen
is removed from the gas at a sufficiently high rate, composition
changes in the boundary layer can cause the sulfur activity of the gas
at the metal surface to increase while the oxygen activity simultaneously
decreases. Figure 7 shows the reaction path for such a situation; a
metal-oxygen-sulfur system in which only metal, oxide MO, and sulfide
MS can exist has been assumed for simplicity. The coordinates are the
chemical potentials μ_0 and μ_S of oxygen and sulfur. The stability fields
for each possible phase are indicated, and are separated by straight

solid lines which represent the chemical potentials at which two phases
can co-exist. The bulk gas composition has been taken to lie in the MO
stability field. Diffusive transport of oxygen and sulfur through the
boundary layer may, under the appropriate conditions, produce the
reaction path shown, leading to thermodynamic stability of both MO and
MS at the scale surface. Duplex scale formation would be expected under
such conditions.

Many laboratory investigations of oxidation by oxygen and sulfur
have been carried out by using gas mixtures of SO_2 and some inert gas
such as Ar. Duplex oxide/sulfide scale formation can be achieved readily
over a range of SO_2 concentrations and temperatures, but tends to reach
a maximum rate for an intermediate SO_2 concentration. To determine if
this result were likely to be a consequence of known factors rather than
some property of the oxide or sulfide, the diffusive transport of oxygen
and sulfur through the boundary layer was examined. In particular, the
conditions for a sulfur activity increase leading to sulfide formation
at the surface of an existing oxide scale were considered since a pre-
existing oxide layer will prevent duplex scale formation if sufficiently
thick.

Figure 8 shows schematically the gas phase compositions through
the boundary layer of thickness δ adjacent to metal covered with an
oxide layer of thickness L for the condition where net sulfur transport
is zero, but the sulfur activity has just risen to the point where sulfide
will be stable at the oxide surface. The SO_2 and O_2 contents of the

bulk gas are the mole fractions $x_{SO_2}^b$ and $x_{O_2}^b$, respectively. This O_2 content of the bulk gas in a laboratory experiment will depend on the purities of the SO_2 and inert gas used; while the inert gas can be purified to very low O_2 levels, the SO_2 will contain some residual O_2 in amounts up to 1000 ppm[13]. At the oxide/gas interface, the SO_2 content of the gas is essentially unchanged, while the O_2 content has dropped to $x_{O_2}^i$ and the S_2 content has rise from a near-zero value in the bulk gas to a value of $x_{S_2}^i$. Cation transport of metal through the oxide to the oxide/gas interface where metal-oxygen reaction actually occurs is responsible for the gradient in O_2 content.

In order for sulfide to be stable at the oxide surface, the oxide thickness must be less than some critical value, denoted by L_c. Thicker oxide layers result in cation transport which is too low to support the required decrease in O_2 content that will allow the sulfur activity to increase at the oxide surface. For cation transport via singly charged vacancies, a straightforward mass transport balance, together with the thermodynamic condition for simultaneous oxide/sulfide co-existence, leads to an expression for the ratio L_c/δ as

$$L_c/\delta \sim \frac{K^{1/6}(x_{SO_2}^b)^{1/6} - (a_0^*)^{1/2}}{x_{O_2}^b - K^{2/3}(x_{SO_2}^b)^{2/3}} \qquad \text{IV-1}$$

where the constant K is given by $K_{MS}/K_{MO}K_{SO_2}$, the equilibrium constants for formation of MS, MO, and SO_2 from the elements, and a_0^* is the oxygen activity at the metal/oxide interface, or $1/K_{MO}$. The proportionality

constant implied by IV-1 contains the appropriate diffusivities for the oxide and gas phases. It is the variation of the ratio L_c/δ with bulk gas SO_2 content that is of interest, however.

Figure 9 is a normalized plot of L_c/δ obtained by assuming that the inert gas and the SO_2 contain 1 and 1000 ppm of O_2, respectively, and by utilizing the equilibrium constants for formation of CoS, CoO, and SO_2 at 800°C. This figure indicates that at both very low and very high SO_2 contents of the gas, a relatively thin layer of pre-existing oxide will prevent sulfide formation at the oxide surface. Intermediate SO_2 contents, however, require the thickest preexisting oxide layer to suppress formation of duplex oxide/sulfide scales. Once sulfide stability at the oxide surface has been reached, the rates of formation of oxide and sulfide, and thus the amounts of each formed, will be determined by metal transport in the sulfide as well as the oxide, and the preceding analysis no longer applies. It is thus concluded that initiation of duplex oxide/sulfide scale formation can be accounted for by expected transport and thermodynamic porperties of the oxide and gas phases.

C. Sulfur Transport Through Scale

While gas phase transport conditions may lead to duplex oxide/sulfide scale formation, an increase in sulfur activity through an oxide scale is required to explain formation of sulfide at a metal/oxide interface in an atmosphere which has a sulfur activity below that of the metal/sulfide equilibrium. This situation would lead to a reaction path such as shown

in Fig. 10, where a negligible change in oxygen and sulfur activities across the gas phase boundary layer has been assumed. Reaction paths for activities across a scale in the simultaneous presence of oxygen and sulfur have usually been presented with the sulfur activity or potential decreasing toward the metal/scale interface; an exception is for a scale which may contain pores[11]. The gas reaching such pores, through fissures in the scale which are presumably associated with the pores, loses oxygen with an accompanying rise in sulfur activity. An analogous mechanism for a rise in carbon activity across the oxide scales formed during oxidation of Fe by CO_2 has been demonstrated[14]. There is little evidence that oxide scales formed in O_2 - SO_2 atmospheres contain pores which could similarly cause an increase in sulfur activity across the scale. And if only narrow fissures through the scale are present, removal of oxygen from the gas penetrating these implies their closure by oxide formation. Further, an increase in sulfur activity across a scale due to gas reaching pores does not account for increases observed in the oxidation rate even when no duplex oxide/sulfide scale is present[15].

It is then appropriate to consider the related questions of whether sulfur-induced defects in a growing oxide can lead to an increase in sulfur activity at the metal/oxide interface, and also lead to an increase in oxidation rate without the formation of duplex scales. Rather than select a particular oxide, the prototypical metal deficit oxide MO having properties representative of real oxides will be examined.

1)   Oxidation Rate in the Absence of Sulfur

It will be assumed that the principal defects in the oxide MO
are singly charged metal vacancies. The concentration of these
at an oxide surface exposed to some fixed oxygen activity is then
determined by the equilibrium

$$1/2 \ O_2(g) \ \underset{\leftarrow}{\rightarrow} \ O^= \ \Big| \ {}^x_0 \ + \ V'_M \ + \ h^{\cdot} \qquad\qquad \text{IV-a}$$
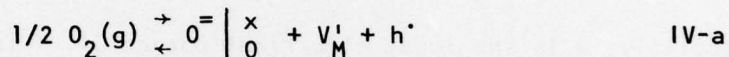
where the symbols have the same significance as for the prototypical
equilibrium discussed in Section I. Letting K_0 denote the equilibrium
constant for IV-a, the concentrations of cation vacancies and electron
holes are related by

$$K_0 = x_v x_h / a_0 \qquad\qquad \text{IV-2}$$

where x_v and x_h are the mole fractions of vacancies and electron holes,
respectively.

Only cation vacancies and electron holes are considered to have
an appreciable mobility in the oxide. The transport equations for
the fluxes of electron holes and vacancies, Γ_h and Γ_v, respectively,
through an oxide of thickness L can be written as

$$L \ \frac{\Gamma_h}{c} \ = \ -\beta_h x_h \ \left(RT \ \frac{d\ln x_h}{d\lambda} \ + \ F \ \frac{dU}{d\lambda}\right) \qquad\qquad \text{IV-3}$$

and

$$L \frac{\Gamma_V}{c} = - \beta_V x_V \left(RT \frac{d\ln x_V}{d\lambda} - F \frac{dU}{d\lambda} \right)$$ IV-4

where λ is a normalized distance through the oxide (distance divided by L), β_h and β_V are the mobilities of electron holes and vacancies, respectively, U is the local electrical potential, T is the absolute temperature, R is the gas constant, F is the Faraday, and c is the concentration of cation sites in the oxide. With this formulation, the mobility of any entity is proportional to its diffusivity; the Nernst-Einstein relation gives the proportionality constant as 1/RT.

Two conditions applicable to the oxide are the requirements for local electroneutrality and for zero net current density. These conditions can be expressed as

$$x_h - x_V = 0$$ IV-5

and

$$\Gamma_h - \Gamma_V = 0$$ IV-6

respectively, for the prototypical oxide.

The three equations IV-2, IV-5 and IV-6 can be used to obtain three simultaneous first order ordinary differential equations in the variables x_h, x_V, and U. While IV-2 and IV-5 can be differentiated directly, IV-3 and IV-4 can be substituted into IV-6 to obtain the

differential form. The three differential equations are

$$d\ln x_h + d\ln x_V = d\ln a_0 \qquad\qquad \text{IV-7a}$$

$$x_h d\ln x_h - x_V d\ln x_V = 0 \qquad\qquad \text{IV-7b}$$

$$-RT \beta_h x_h d\ln x_h + RT \beta_V x_V d\ln x_V - F(\beta_h x_h + \beta_V x_V)dU = 0 \qquad \text{IV-7c}$$

Equations IV-7a through IV-7c allow evaluation of the derivatives $d\ln x_h/d\ln a_0$, $d\ln x_V/d\ln a_0$, and $dU/d\ln a_0$ at any values of x_h and x_V. Since U does not appear explicitly in these equations, the absolute value of the electrical potential cannot be determined, and U may be given any convenient value at some corresponding value of a_0.

For a growing oxide, a_0^b will be used to denote the oxygen activity in the bulk gas to which the oxide is exposed, and a_0^* is the oxygen activity at the metal/oxide interface. Calculation of the values of x_h, x_V, and U at any point within the oxide then becomes an initial value integration problem: IV-2 and IV-5 are used to obtain the values of x_h and x_V at the oxide/gas interface where the oxygen activity is a_0^b, U can be assigned a value of zero at this interface, and integration of the three above derivatives is carried out from a_0^b to any desired oxygen activity greater than or equal to a_0^*. It is convenient to let the quantity RT/F, with the dimensions of volts, be represented by ψ; then U can be expressed as the dimensionless ratio U/ψ.

The metal flux through the growing oxide is equal in magnitude to the vacancy flux, but with the opposite sign. Since there are no sources or sinks of metal within the oxide, the metal flux must be constant across the oxide, and independent of the normalized distance λ.

A quantity D, with the dimensions of a diffusivity, can then be defined as

$$D = - \int_0^1 L \frac{\Gamma_v}{c} d\lambda \qquad\qquad \text{IV-8a}$$

or, from IV-4, and assuming that β_v is constant across the oxide,

$$D = RT \beta_v \int_{a_0^*}^{a_0^b} x_v \left(\frac{d\ln x_v}{d\ln a_0} - \frac{1}{\psi} \frac{dU}{d\ln a_0} \right) d\ln a_0 \qquad \text{IV-8b}$$

It is apparent that D, which is directly proportional to the metal flux and inversely proportional to the oxide thickness, will be related to a rate constant for oxidation. Since D is independent of λ, it must also be independent of a_0. Then in principle its value could be obtained at any single point within the oxide. The integral formulation of IV-8 avoids the necessity for selecting such a point.

This prototypical example actually can be solved in closed form, and leads to the well-known situation of parabolic oxidation. The quantity D is given by

$$D = 1/2 (W_{MO}/\rho_{MO}W_0)^2 k_p \qquad\qquad \text{IV-8c}$$

where W_{MO} and W_0 are the molecular weights of MO and O, respectively, ρ_{MO} is the density of MO, and k_p is the parabolic rate constant for weight gain. D can also be expressed as

$$D = 2RT \beta_v k_0^{1/2} \left[(a_0^b)^{1/2} - (a_0^*)^{1/2} \right] \qquad \text{IV-8d}$$

for the condition that $\beta_h \gg \beta_v$. More complex situations, however,
can be treated by the same approach of formulating the appropriate
differential equations and integrating over a_0. If metal transport
takes place only by vacancy motion, equation IV-8b will still yield
the correct value for D. In particular, if additional defects which
do not cause metal transport are to be considered, then the value of
D can be compared to a reference value D° evaluated in the absence
of such defects and integrated over the limits of 0 and 1. Thus for the
prototypical oxide MO, D° is given by

$$D^\circ = 2RT \, \beta_v K_0^{1/2} \qquad\qquad IV-9$$

again subject to the condition that $\beta_h \gg \beta_v$.

The variation of x_h, x_v, and U across the oxide MO are shown in
Fig. 11, where K_0 has been taken as 10^{-8} and a_0^b is unity (1 atm O_2).
The cation vacancy and electron hole concentrations are equal, to satisfy
the electroneutrality and zero net current conditions. It was assumed
that electron hole mobility was much greater than vacancy mobility.
While both electron holes and vacancies flow down their respective
concentration gradients, the electrical potential assists the motion
of negatively charged vacancies and opposes the motion of positive
electron holes.

2)   Oxidation Rate in the Presence of Sulfur

It might be expected that the electrical potential would affect
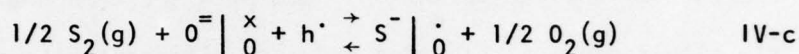the distribution of sulfur-induced defects. The present work indicates

that at high O_2 partial pressures, such defects do not greatly influence oxide conductivity. Thus the majority of these cannot carry any excess charge. Other work, however, suggests that sulfur enters metal oxides as an electron donor to reduce the electron hole concentration; this behavior may reflect a sulfur-induced defect present at low O_2 partial pressures[15,16]. Therefore two types of sulfur-induced defect in oxide MO were postulated.

The first defect is the type suggested by this study, and consists of S^{++} ions on cation sites. The equilibrium governing these is

$$1/2 \ S_2(g) + V_M' + h^{\cdot} \ {\overset{\rightarrow}{\underset{\leftarrow}{}}} \ S^{++} \Big|_M^x \qquad \qquad IV\text{-}b$$

This defect, with a concentration x_S', would have no effect on electrical conductivity (since the hole concentration is still determined by IV-2), and is assumed to have a constant mobility of 10 times less than the vacancy mobility. The ionic radius of S^{++} ions, which would determine whether such defects are physically reasonable, is difficult to evaluate since few solid compounds contain this ion. The ionic radius of sulfur decreases in going from S° to S^{4+}, and it would be expected that S^{++} follows this trend. While the experimental observations of the present work regarding mobility of sulfur-induced defects at high O_2 pressure depends upon a slight increase in conductivity due to these defects, it also appears that only a small fraction of such defects are affecting the conductivity. Thus the postulated defect has zero excess charge.

The second defect has been suggested previously as noted, and consists of S^- ions on anion sites. The equilibrium governing these is

$$1/2\ S_2(g) + O^= \left|\begin{matrix} x \\ O \end{matrix}\right. + h^\cdot \overset{\rightarrow}{\underset{\leftarrow}{}} S^- \left|\begin{matrix} \cdot \\ O \end{matrix}\right. + 1/2\ O_2(g) \qquad \text{IV-c}$$

This defect, with a concentration x_S'', would decrease electrical conductivity, especially at low O_2 partial pressures, and is assumed to have a constant mobility 10^4 times less than the vacancy mobility. This mobility is based on the low self-diffusion coefficient observed for oxygen in metal-deficit oxides.

The equilibrium constants for the two postulated defects are

$$K_S' = X_S'\ /a_S x_v x_h \qquad \text{IV-10}$$

and
$$K_S'' = x_S'' a_O /a_S x_h \qquad \text{IV-11}$$

Equations IV-10 and IV-11 can be differentiated directly. The fluxes Γ_S' and Γ_S'' for the two sulfur-induced defects can be expressed in a form similar to that of IV-4. The conditions of local electroneutrality and zero net current density still apply to the oxide containing sulfur-induced defects. An independent specification of the sulfur flux is required for complete definition of the problem, however. An appropriate condition is that the total sulfur flux, the sum of Γ_S' and Γ_S'', be zero. If the sulfur activity at the metal/oxide interface is less than the value required to form sulfide, then the metal will not constitute a sink for sulfur and no sulfur transport will occur. Imposing a zero

net sulfur flux will allow determination of the sulfur activity that can be attained. Once sulfide stability is reached, a net sulfur flow will occur and a different anlysis would have to be considered to determine the rate of sulfide formation. But with the zero net sulfur flux specified, six simultaneous first order ordinary differential equations analogous to IV-7 can be obtained in the variables x_h, x_v, U, x_S', x_S'', and a_S. Calculation of these again becomes an initial value integration problem, with the integration taking place over oxygen activity from a_0^b to a_0^*. Neglecting any possible metal transport by the first type of sulfur-induced defect, the value of D can still be obtained from IV-8b. The differential equations can no longer be solved in closed form, and a numerical integration procedure capable of handling moderately stiff equations must be employed.

Table IV.1 presents the results of solutions obtained at several values of the bulk sulfur activity a_S^b (which is an initial condition for the integration). Other initial conditions at the oxide/gas interface are: $a_0^b = 0.1$ and values of $x_S' = 1.3 \times 10^{-5}$ and $x_S'' = 2.8 \times 10^{-7}$ for the specific case of $a_s^b = 10^{-10}$. These latter two conditions are consistent with the assumed properties of the sulfur-induced defects, while the bulk gas oxygen and sulfur activities selected for calculations represent a gas with 1% O_2 and an SO_2 content ranging from very low to about 10%. In Table IV.1, x_S^i, x_v^i, and U^i are the values of these quantities at the metal/oxide interface, and $D/D°$ is the ratio of D to $D°$ calculated from IV-9. The value of K_0 was again taken as 10^{-8}, leading to a vacancy concentration at the oxide/gas interface of 3.16×10^{-5}.

Table IV.1

a_S^b	a_S^i	x_V^i	U^i/ψ	D/D°
10^{-18}	2.04×10^{-19}	1.00×10^{-8}	7.90	0.319
10^{-16}	2.04×10^{-17}	8.91×10^{-9}	7.79	0.319
10^{-14}	2.51×10^{-15}	1.29×10^{-9}	5.87	0.322
10^{-13}	8.71×10^{-11}	2.88×10^{-6}	6.85	0.347
10^{-12}	3.63×10^{-8}	5.75×10^{-5}	7.61	0.370
10^{-11}	3.89×10^{-6}	5.89×10^{-4}	8.72	0.411
10^{-10}	2.45×10^{-4}	4.68×10^{-3}	9.63	0.487

One feature of Table IV.1 is immediately apparent: the postulated
defects lead to an increase in metal/oxide interface sulfur activity
over that of the bulk gas at sulfur activities exceeding about 5×10^{-14},
as well as to an increase in parabolic oxidation rate constant (as
reflected by D/D°, recognizing that $D/D^\circ = 0.319$ for the limiting case
of $a_S^b = 0$, $a_O^b = 0.1$). It is also apparent that these results are not
simply explicable. The electrical potential at the metal/oxide interface
first decreases with bulk sulfur activities, and then increases. At
bulk sulfur activities of 10^{-12} or higher, the vacancy concentration
at the metal/oxide interface exceeds that at the oxide/gas interface.
Thus cation vacancies are diffusing up their concentration gradient,
with a resulting parabolic oxidation rate constant that is higher than
if they had been diffusing in a "normal" manner. Presumably the
electrical potential still affects vacancy motion, but a conclusion
is that multiple defect interactions must be treated as rigorously as

possible to obtain correct results regarding effects on chemistry and kinetics.

The conditions leading to the results of Table IV.1 were not chosen to obtain predetermined values. The sulfur-induced defects were modelled in view of existing experimental evidence. Different concentrations and mobilities of the sulfur-induced defects lead to somewhat different but generally similar results. Other types of sulfur-induced defects can be postulated, of course, leading to completely different results. The success of the postulated sulfur-induced defects at accounting for an increase in sulfur activity across a growing oxide and an increase in parabolic oxidation cannot be taken to mean that such defects exist. The prototypical oxide examined here has in effect been considered as a single crystal; grain boundary defects may well overwhelm any lattice defects, though the former could presumably lead to many of the same results as the postulated lattice defects. This examination of possible defect interactions in a growing oxide exposed to a sulfur-containing atmosphere does show that values of sulfur activity or potential along the reaction path across the oxide cannot be assumed to simply remain equal to the bulk gas value or even decrease.

V. Conclusions

1) At high O_2 partial pressures, exposure of intrinscially conducting single crystal NiO and CoO to SO_2 results in small conductivity increases of the order of 1% at 1000°C.

2) The apparent diffusivity of defects in single crystal NiO and CoO which have been exposed to SO_2, as measured by conductivity

variation with time following a change in O_2 partial pressure, shows a decrease at long times that appears to be associated with a sulfur-induced defect.

3)   Thermogravimetric measurements indicate a sulfur solubility of about 0.05 mole percent in CoO exposed to O_2 - 2% SO_2 at 1000°C.

4)   Theroetical considerations show that the presence of a lattice defect induced by sulfur, and having properties consistent with the above observations, can lead to an increase in sulfur activity or chemical potential across a growing layer of metal-deficit oxide.

The above conslusions suggest that, at high O_2 partial pressures, the principal sulfur-induced defect in divalent metal-deficit oxide may be an S^{++} ion occupying a cation site. The existence of such a defect would not rule out the existence of other sulfur-induced defects at low O_2 partial pressures.

-40-

ACKNOWLEDGEMENTS

The authors wish to express their appreciation to K. L. Luthra
for generating the computer programs for treatment of mass data on CoO.

REFERENCES

1. W. Jost, Diffusion, Academic Press, Inc., New York (1960).

2. P. Kofstad, Nonstiochiometry, Diffusion, and Electrical Conductivity in Binary Oxides, Wiley Interscience, New York (1972).

3. Y. Ikeda and K. Nii, Trans. Japan, Inst. Met., 17, 419 (1976).

4. S. Mitoff, J. Chem. Phys., 35, 882 (1961).

5. J. B. Wagner, Jr., "Chemical Diffusion Coefficients for Some Nonstiochiometric Metal Oxides", in NBS Spec. Pub. 296, U.S. GPO, Washington (1968).

6. S. Mrowec and K. Przybylski, Oxid. Metals, 11, 383 (1977).

7. R. H. Chang, Ph.D. Thesis, Northwestern Univ. (1973).

8. N. Birks, priv. comm., from M. C. Pope, Ph.D. Thesis, Sheffield Univ. (1975).

9. A. Rahmel, Corr. Science, 13, 125 (1973).

10. N. Birks, in High Temperature Gas-Metal Reactions in Mixed Environments, TMS-AIME, 1972, S. A. Jansson and Z. A. Foroulis (ed), ASM (1973).

11. P. L. Hemmings and R. A. Perkins, Interim Report EPRI FP-539, Electric Power Res. Inst., Palo Alto (1977).

12. W. L. Worrell and H. I. Kaplan, "Dissociation of Gaseous Molecules on Solid Surfaces at Elevated Temperatures", in Heterogeneous Kinetics at Elevated Temperatures, Plenum Press, New York (1970).

13. Based on supplier specification of SO_2 of 99.9 to 99.98% purity.

14. J. D. Noden et. al., Brit. Corr. J., 3, 47 (1968).

15. V. N. Konev, et. al., Zaschita Metallov., 6, 448 (1970).

16. G. Romeo, H. S. Spacil, and W. J. Pasko, J. Elec. Soc., 122, 329 (1975).
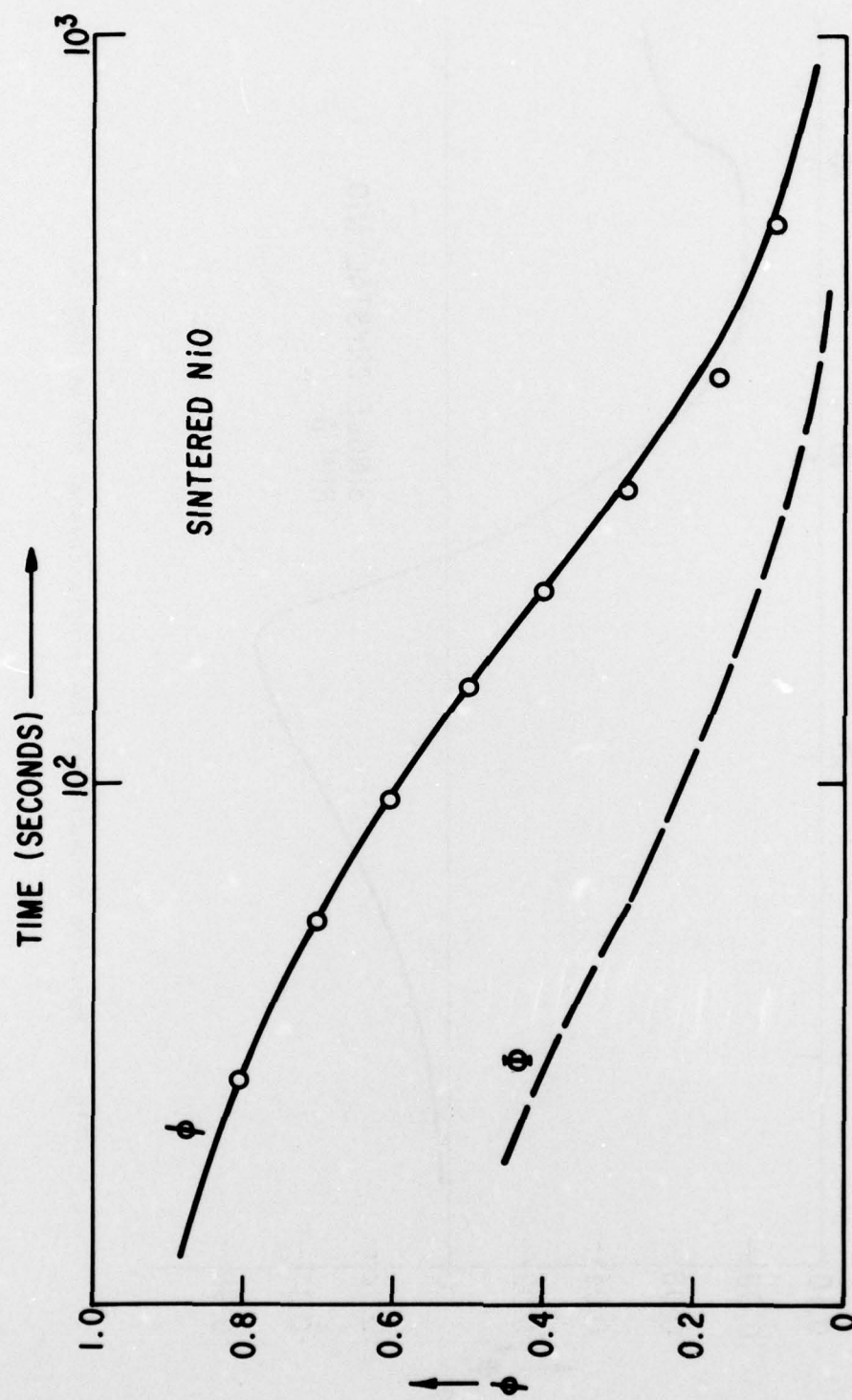
Fig. 1 Normalized conductivity (ϕ, solid line) and normalized surface vacancy concentration (Φ, dashed line) for polycrystalline NiO at 800 °C. Circles are calculated values.
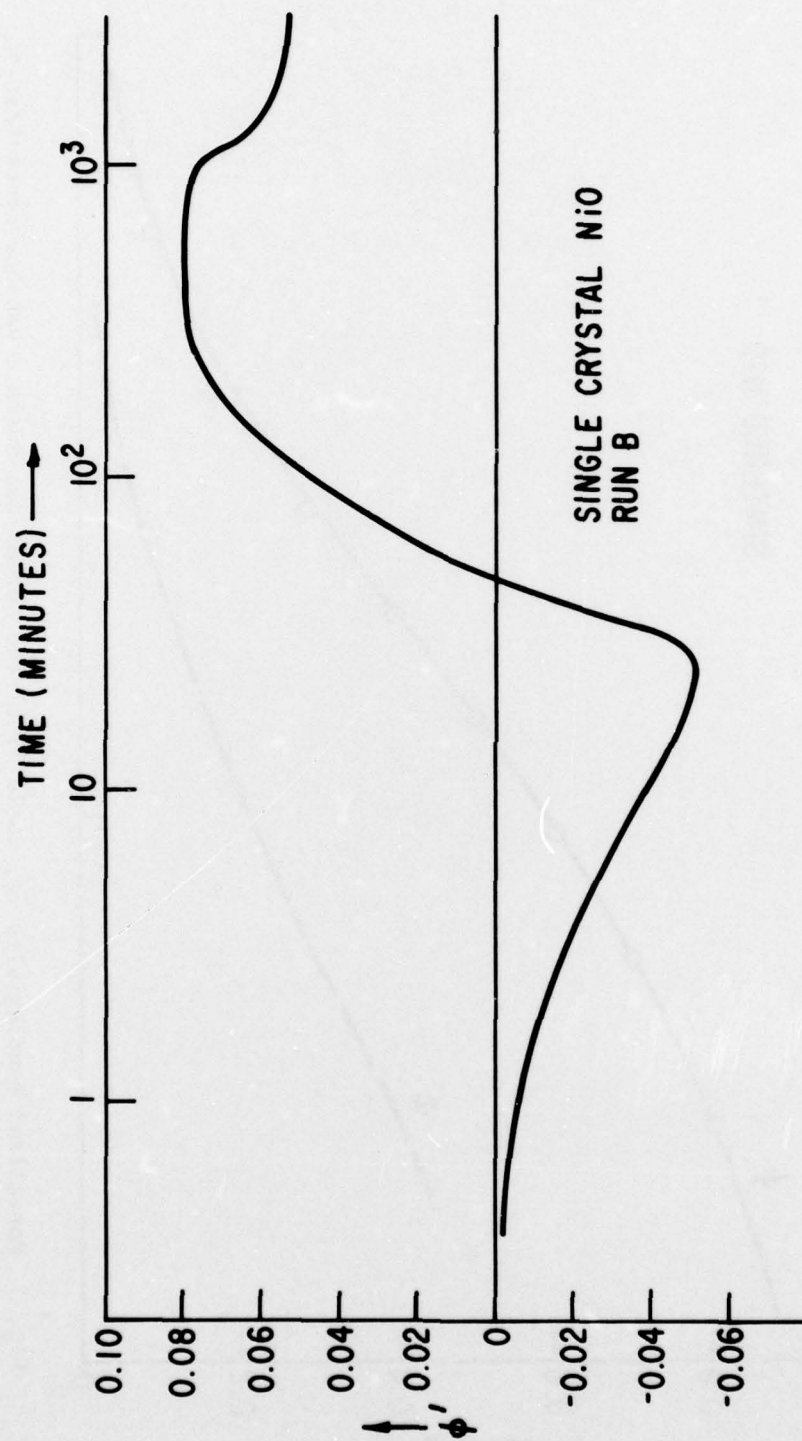
-44-

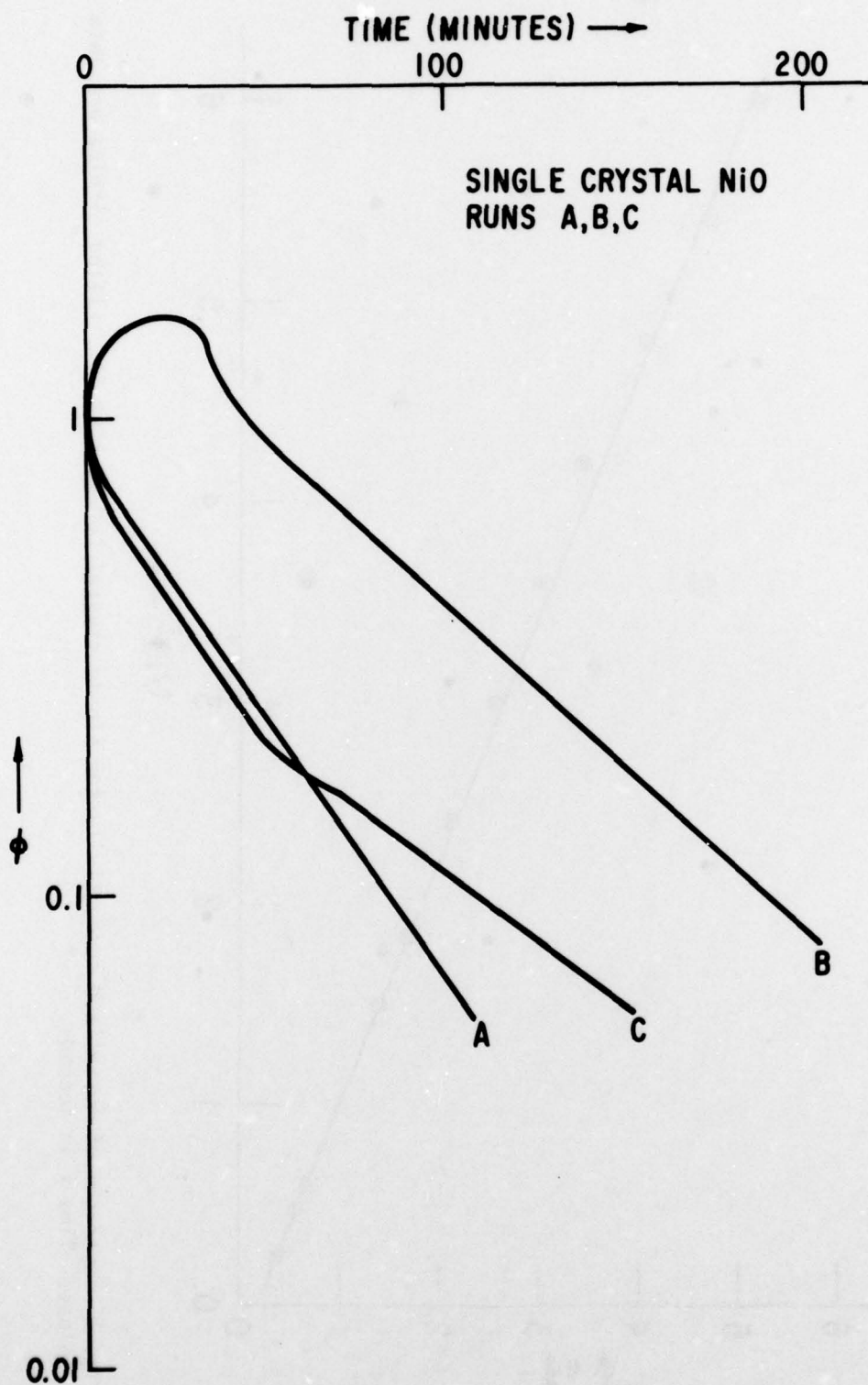Fig. 2 Relative conductivity for single crystal NiO at 1000 °C.

Fig. 3 Normalized conductivity for single crystal NiO at 1000 °C.

Fig. 4 Logarithm of normalized conductivity for single crystal CoO at 1000 °C. Filled circles are data points. Time t in seconds.
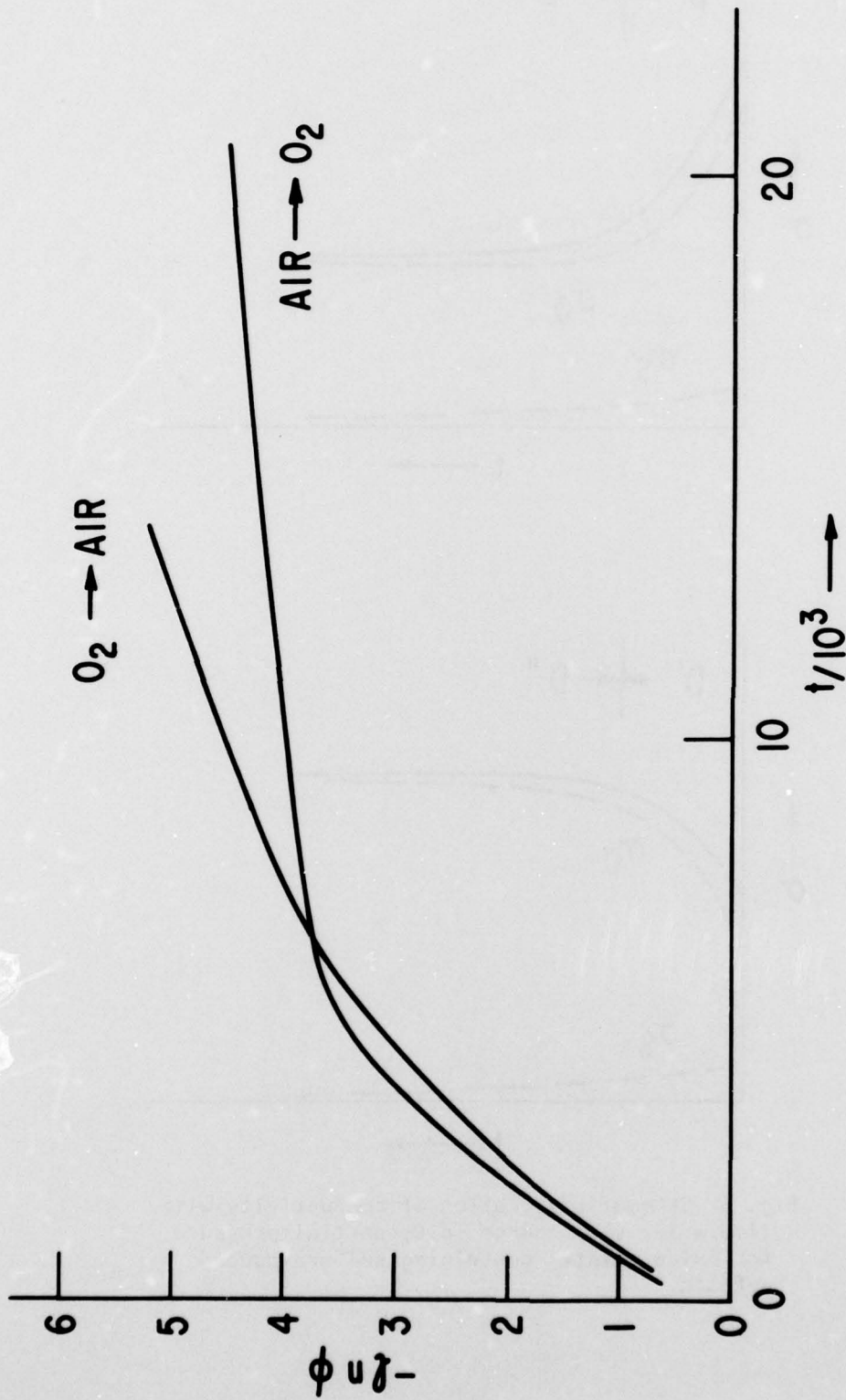
Fig. 5 Logarithm of normalized conductivity for single crystal CoO at 1000 °C after exposure to $O_2 - SO_2$. Time t in seconds.
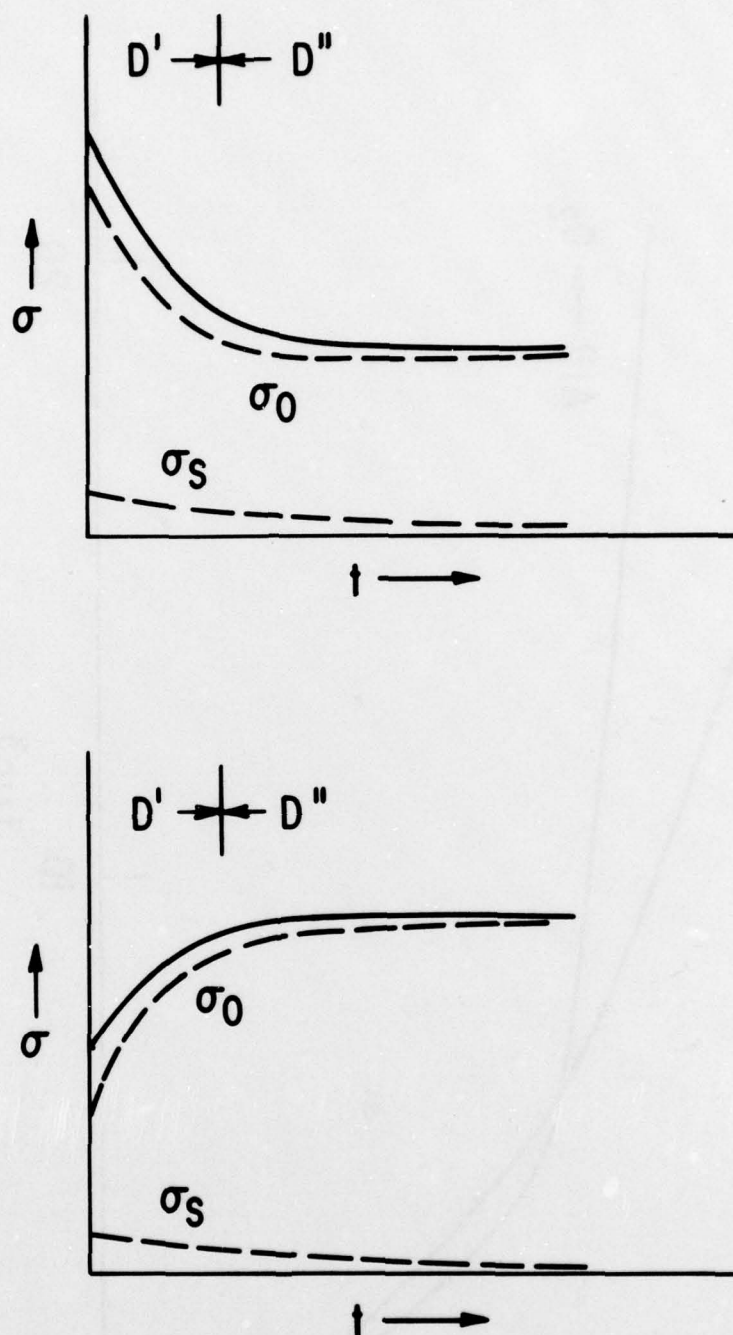
Fig. 6 Schematic variation of conductivity with
time after step change in O_2 partial pressure
for oxide crystal containing sulfur-induced
defects.
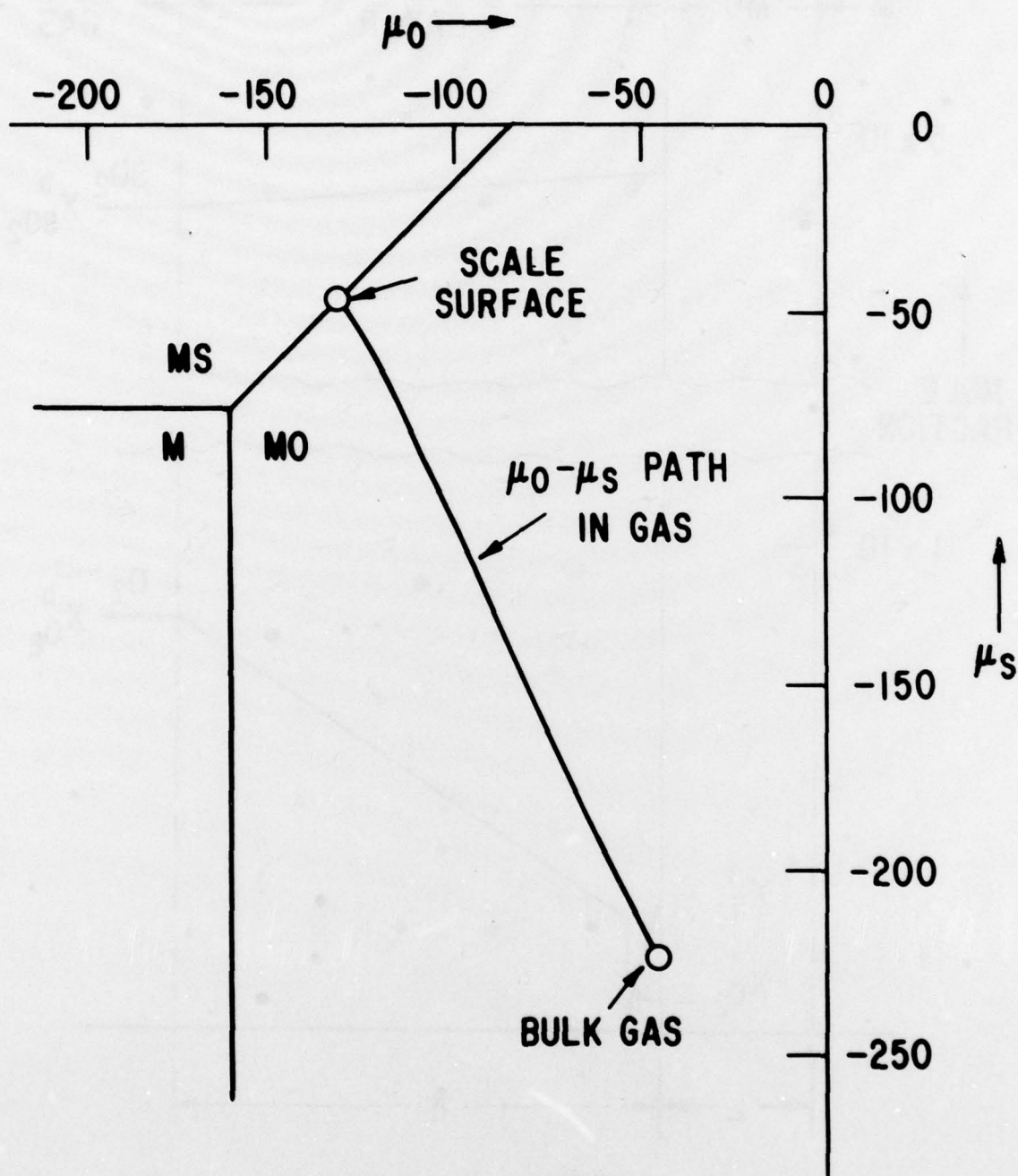
Fig. 7 Reaction path for formation of duplex oxide/sulfide scales by increase of sulfur potential in gas phase boundary layer.
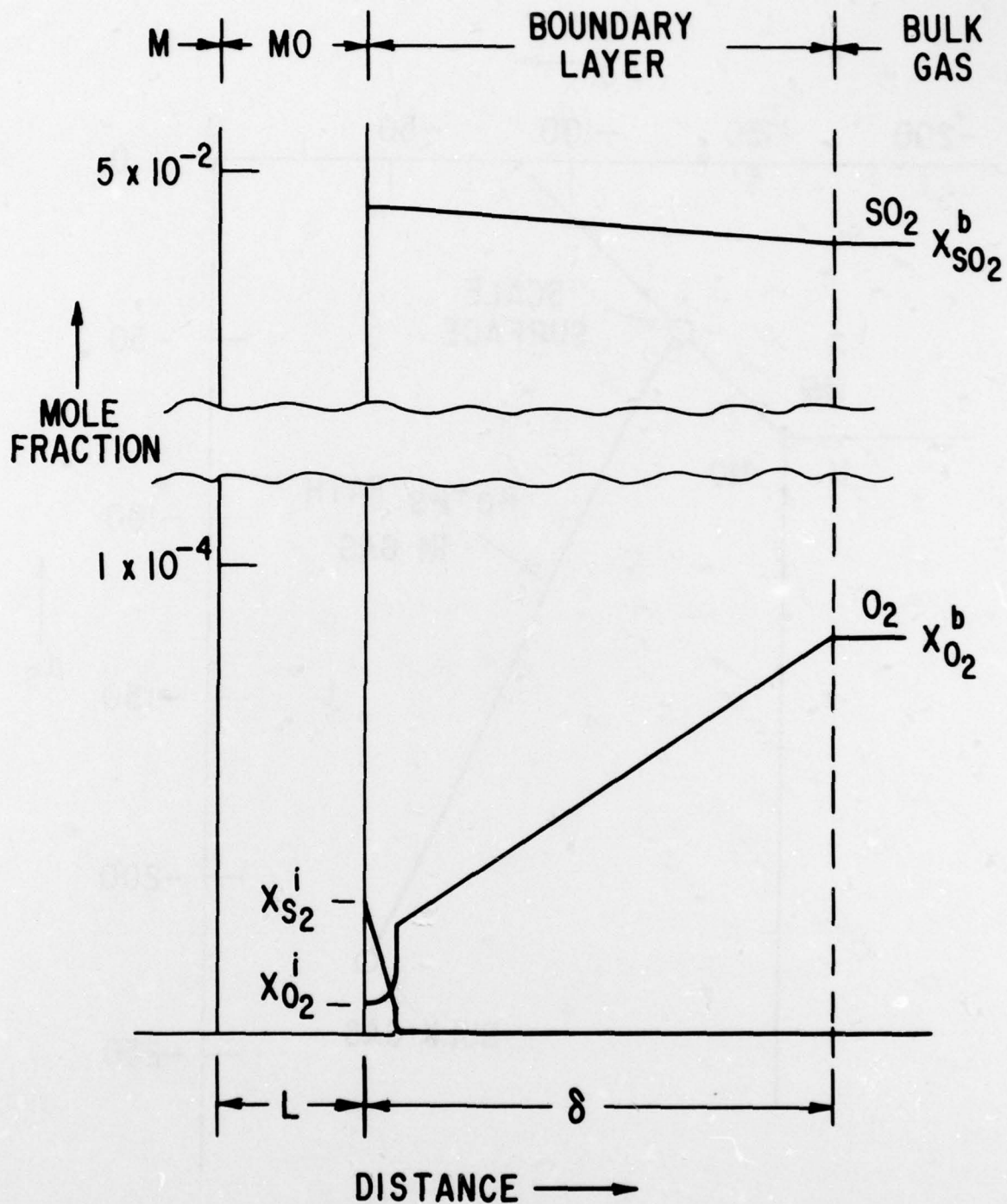
Fig. 8 Composition gradients across gas phase boundary layer prior to formation of duplex oxide/sulfide scale.
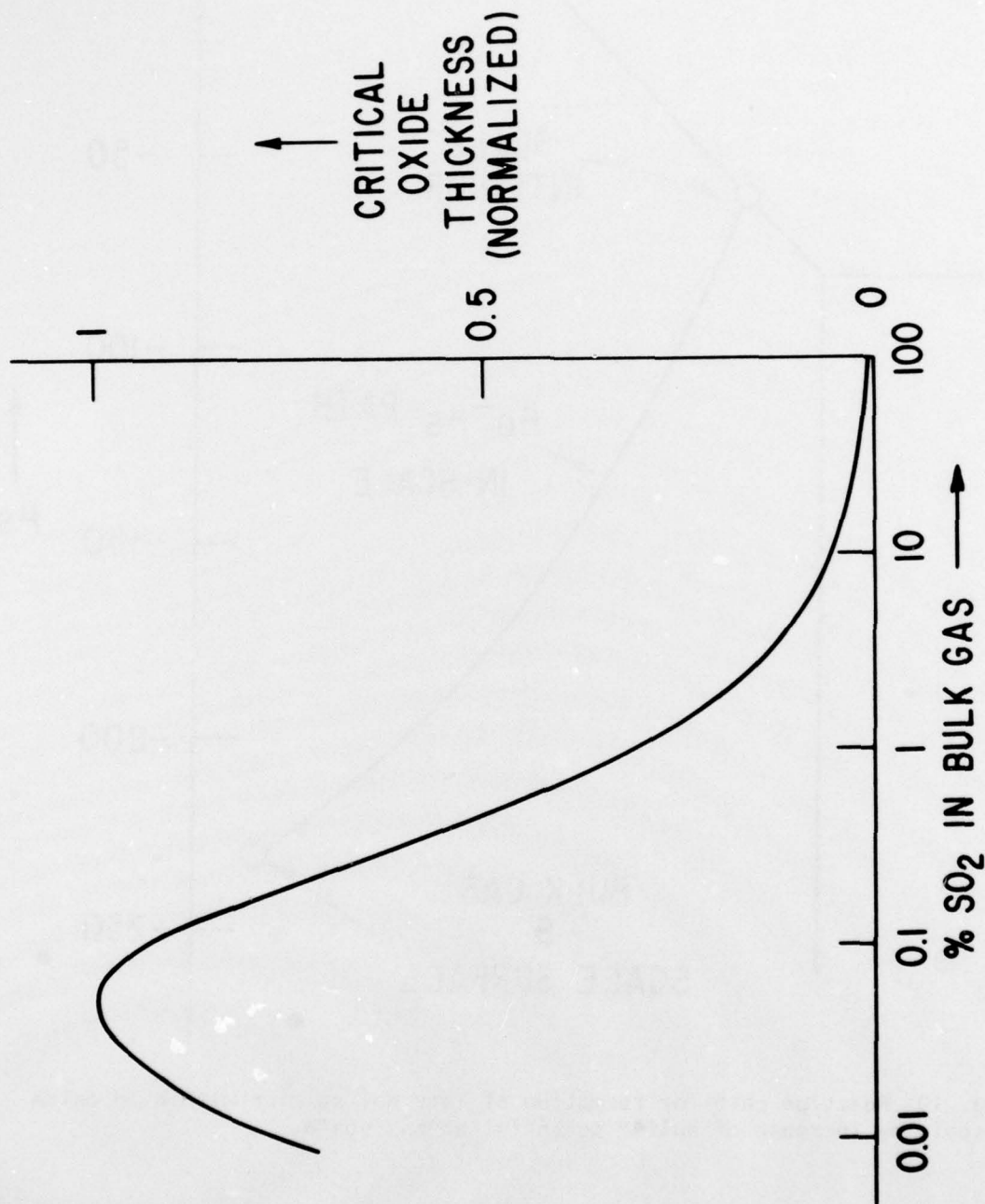
Fig. 9 Normalized critical oxide thickness for formation of duplex oxide/sulfide scales as a function of gas phase SO2 content.
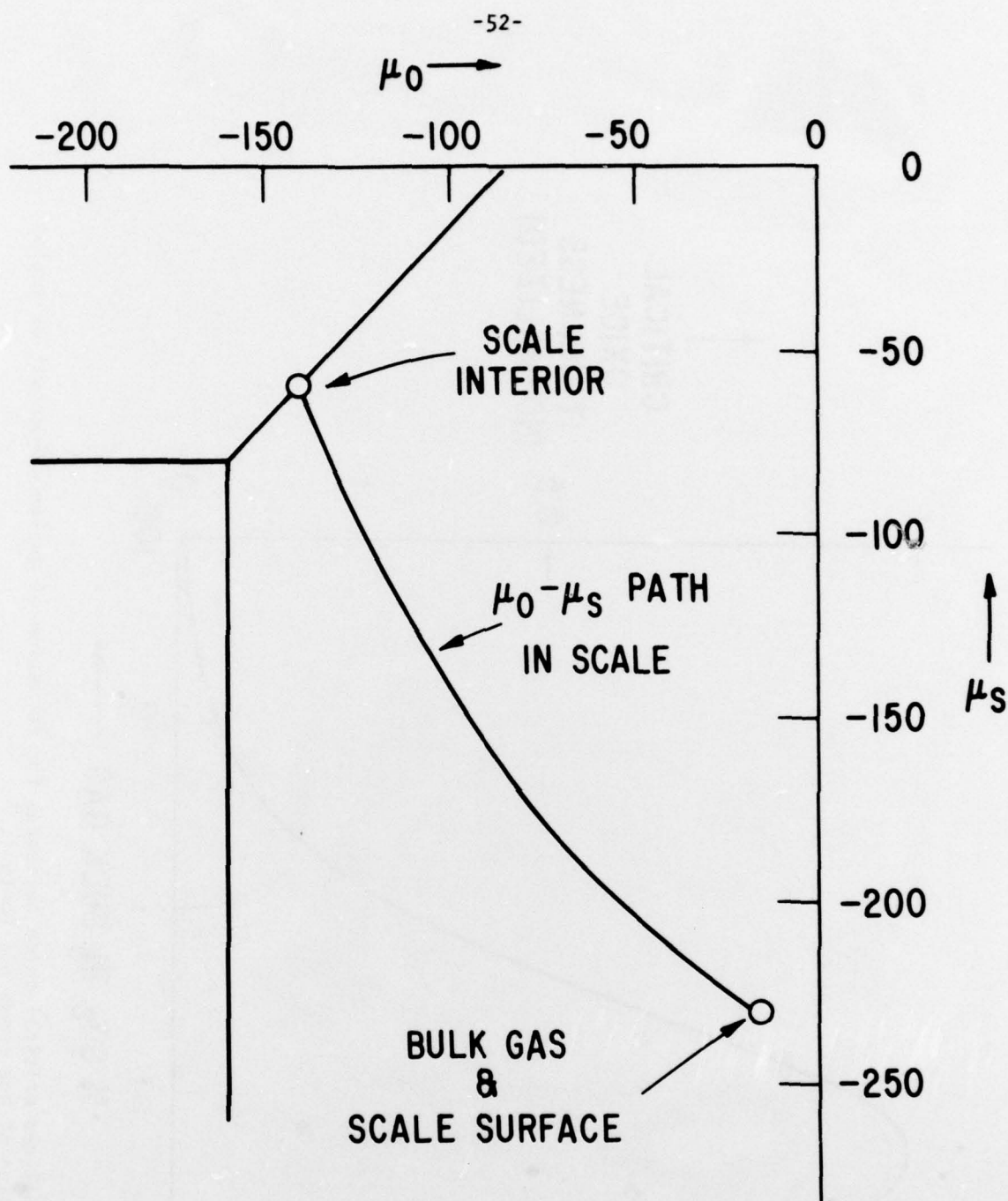
Fig. 10 Reaction path for formation of internal sulfide within an oxide scale by increase of sulfur potential across scale.
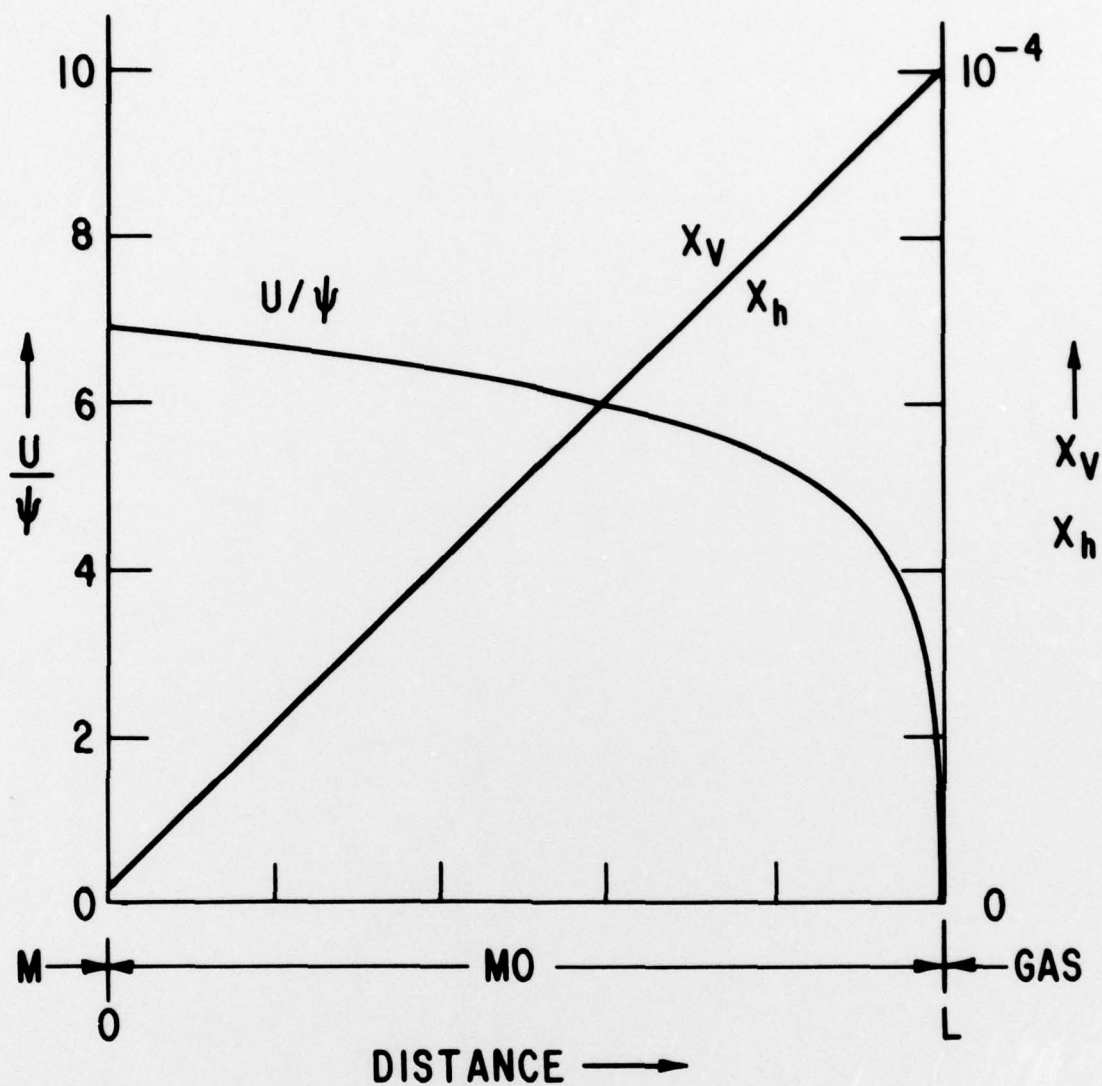
Fig. II Cation vacancy and electron hole concentrations, and electrical potential across growing oxide scale. Concentrations are as mole fraction, and ψ is the quantity RT/F.